

Photochemical & Photobiological Sciences

Accepted Manuscript



This article can be cited before page numbers have been issued, to do this please use: X. Zheng, S. M. Baumann, S. M. Chintala, J. B. Slaughter, K. D. Galloway and R. D. McCulla, *Photochem. Photobiol. Sci.*, 2016, DOI: 10.1039/C5PP00466G.



This is an *Accepted Manuscript*, which has been through the Royal Society of Chemistry peer review process and has been accepted for publication.

Accepted Manuscripts are published online shortly after acceptance, before technical editing, formatting and proof reading. Using this free service, authors can make their results available to the community, in citable form, before we publish the edited article. We will replace this *Accepted Manuscript* with the edited and formatted *Advance Article* as soon as it is available.

You can find more information about *Accepted Manuscripts* in the [Information for Authors](#).

Please note that technical editing may introduce minor changes to the text and/or graphics, which may alter content. The journal's standard [Terms & Conditions](#) and the [Ethical guidelines](#) still apply. In no event shall the Royal Society of Chemistry be held responsible for any errors or omissions in this *Accepted Manuscript* or any consequences arising from the use of any information it contains.



Journal Name

ARTICLE

Photodeoxygenation of dinaphthothiophene, benzophenanthrothiophene, and benzonaphthothiophene S-oxides

X. Zheng, S. M. Baumann, S. M. Chintala, K. D. Galloway, J. B. Slaughter, and R. D. McCulla^aReceived 00th January 20xx,
Accepted 00th January 20xx

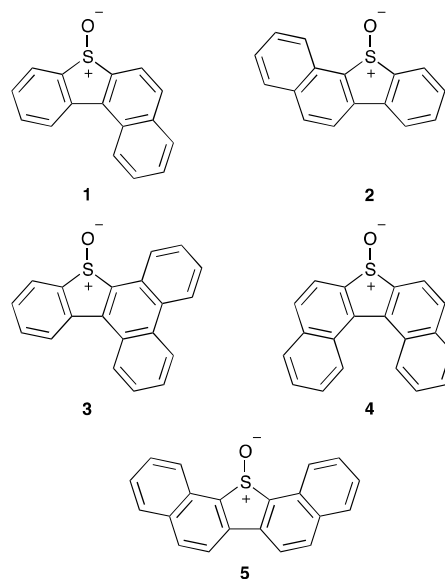
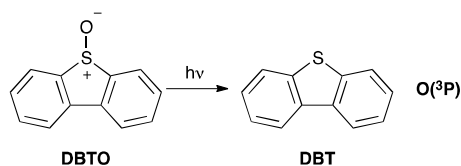
DOI: 10.1039/x0xx00000x

www.rsc.org/

Photoinduced deoxygenation of dibenzothiophene S-oxide (DBTO) has been suggested to release atomic oxygen [$O(^3P)$]. To expand the conditions and applications where $O(^3P)$ could be used, generation of $O(^3P)$ at longer wavelengths was desirable. The sulfoxides benzo[b]naphtho-[1,2,d]thiophene S-oxide, benzo[b]naphtho[2,1,d]thiophene S-oxide, benzo[b]phenanthro[9,10-d]thiophene S-oxide, dinaphtho[2,1-b:1',2'-d]thiophene S-oxide, and dinaphtho[1,2-b:2',1'-d]thiophene S-oxide all absorb light at longer wavelengths than DBTO. To determine if these sulfoxides could be used to generate $O(^3P)$, quantum yield studies, product studies, and computational analysis were performed. Quantum yields for the deoxygenation were up to 3 times larger for these sulfoxides compared to DBTO. However, oxidation of the solvent by these sulfoxides resulted in different ratios of oxidized products compared to DBTO, which suggested a change in deoxygenation mechanism. Density functional calculations revealed a much larger singlet-triplet gap for the larger sulfoxides compared to DBTO. This led to the conclusion that the examined sulfoxides could undergo deoxygenation by two different mechanisms.

Introduction

The photodeoxygenation of aromatic heterocyclic oxides, such as dibenzothiophene S-oxide (**DBTO**), is believed to generate ground-state atomic oxygen [$O(^3P)$], and this oxidant displays a reactivity considerably different than other reactive oxygen species (ROS).¹⁻⁷ Specifically, $O(^3P)$ reacts selectively towards a series of small organic molecules, and the photodeoxygenation of a **DBTO** derivative results in the near quantitative oxidation of a specific cysteine residue of the plant protein adenosine-5'-phosphosulfate kinase.^{8,9} The unique selectivity and ability to photorelease $O(^3P)$ raises the possibility of targeting a specific biomolecule for oxidation in a complex mixture; however, the limited number of methods and conditions suitable for the generation of $O(^3P)$ constrains potential applications.



While the photodeoxygenation of **DBTO** is one of the few methods capable of cleanly producing $O(^3P)$ in solution, one limitation of **DBTO** is the need for UV-A irradiation. Absorption of wavelengths above 350 nm by **DBTO** is miniscule. Thus, any sample containing molecules capable of absorbing UV-A irradiation increase the risk of complicating photochemistry. One approach to circumvent this obstacle is to extend the chromophore of **DBTO** in order to red-shift the absorption spectrum. To these ends, the ability of benzo[b]naphtho-[1,2,d]thiophene S-oxide (**1**), benzo[b]naphtho[2,1,d]-

^a 3501 Laclede Ave. St. Louis, MO 63013, rmccull2@slu.edu.

† Footnotes relating to the title and/or authors should appear here.

Electronic Supplementary Information (ESI) available: [details of any supplementary information available should be included here]. See DOI: 10.1039/x0xx00000x

thiophene *S*-oxide (**2**), benzo[b]phenanthro[9,10-d]thiophene *S*-oxide (**3**), dinaphtho[2,1-b:1',2'-d]thiophene *S*-oxide (**4**), and dinaphtho[1,2-b:2',1'-d]thiophene *S*-oxide (**5**) to generate an oxidant similar to the parent **DBTO** is examined in this work.

The irradiation of **2** in 2-methylbutane yields a similar product mixture as **DBTO**, which provides evidence for the generation of a similar oxidant.¹⁻³ Additionally, the photodeoxygenation of **2** can be carried out at wavelengths as high as 385 nm. Production of O(³P) during the photodeoxygenation of **2** is further supported by the similar yields of styrene oxidation products arising from photodeoxygenation of **2** and O(³P) generated by microwave discharge methods (MDM).⁴ Thus, we posit the increased benzannulation of **DBTO** is a promising strategy to achieve the production of O(³P) at wavelengths stretching into the visible spectrum.

Photodeoxygenation of **1-5** is expected to produce an oxidant similar to the parent **DBTO**. While the available evidence suggests the oxidant released by **DBTO** is O(³P), direct detection of O(³P) in solution is challenging due to its reactivity and limited spectral window. Indirect evidence for identity of this oxidant as discrete O(³P) arises from the comparison of products from multiple sources of O(³P), such as the MDM and photodeoxygenation of **2** cited above. Additionally, the oxidant reacts with O₂ to generate O₃ and displays diffusion-limited rate constants of a magnitude only possible for a very small oxidant.^{4,8,10} Regardless of the exact nature of the oxidant, O(³P) is used in this article to refer to the oxidant generated during the photodeoxygenation of **DBTO**.

As discussed earlier, a distinguishing feature of O(³P) is a unique selectivity. For example, hydroxyl radical (•OH) reacts with a large array of organic compounds at nearly diffusion-limited rates; whereas, rate constants for the reaction between O(³P) and the same array of organic compounds spanned over six orders of magnitude.⁸ More recently, this selectivity also extends to biological samples.⁹⁻¹³ In addition to the selective oxidation of cysteine mentioned earlier, photodeoxygenation of a **DBTO** derivative generated fatty aldehydes associated with plasmalogens over other possible unsaturated fatty acids in low-density lipoprotein (LDL).¹¹ The production of O(³P) is also known to induce single-strand cleavage in DNA.^{12,13} These results suggest O(³P) could be used to create specific oxidation products in more complicated biological samples. For these samples, the efficient production of O(³P) at longer wavelengths, where these samples are more transparent, is desirable.

Experimental and Computational Methods

Materials

Commercial materials were obtained from Aldrich, Fisher or AKScientific and used without modification, except as noted. HPLC grade toluene and benzene were used for the solvent oxidation experiments. The corresponding thiophene of compounds **1-4** were prepared according to literature procedure with slight modifications.¹⁴⁻¹⁹ Dinaphtho[1,2-b:2',1'-d]thiophene *S*-oxide (**5**)

was prepared by a new synthetic route. Full details of the sulfoxides **1-5** preparation are given in the electronic supporting information.

General procedure for oxidation of DBT and the corresponding thiophene of 1-5. First, 120.0 mg (0.42 mmol) dinaphtho[1,2-b:2',1'-d]thiophene was dissolved in 100 mL CH₂Cl₂ at -30 °C. Then 127 mg of 77 wt% mCPBA (0.57 mmol) was dissolved in another 100 mL of dichloromethane and added to the reaction mixture dropwise. After the reaction mixture was warmed to room temperature, the reaction mixture was washed with saturated sodium bicarbonate solution. The organic layer was collected, and the aqueous layer was extracted with CH₂Cl₂ three times. The combined organic extracts were dried over Na₂SO₄ and then concentrated under reduced pressure. The crude product was subjected to column chromatography (CH₂Cl₂ as eluent) to afford dinaphtho[2,1-b:1',2'-d]thiophene *S*-oxide (31.2 mg, 0.110mmol, 26.1% yield).

General Methods

Absorption spectra were recorded using a NanoDrop 2000c UV-Vis spectrophotometer using samples contained in 10 × 10 mm quartz cell. NMR spectra were recorded using a Bruker DRX-400 NMR. High-resolution mass spectra were obtained using a JEOL JMS-700 mass spectrometer. An Agilent 1200 Series HPLC fitted with a quaternary pump and diode array detector was used for HPLC chromatographs run on an Agilent Eclipse XDB-C18 column (5µm, 150 × 4.6mm). For gas chromatograph analysis, a Hewlett-Packard 5900 Series GC fitted with a flame ionization detector and a Sciencix CTS-5 column (0.25mm × 30m × 0.25µm) was used.

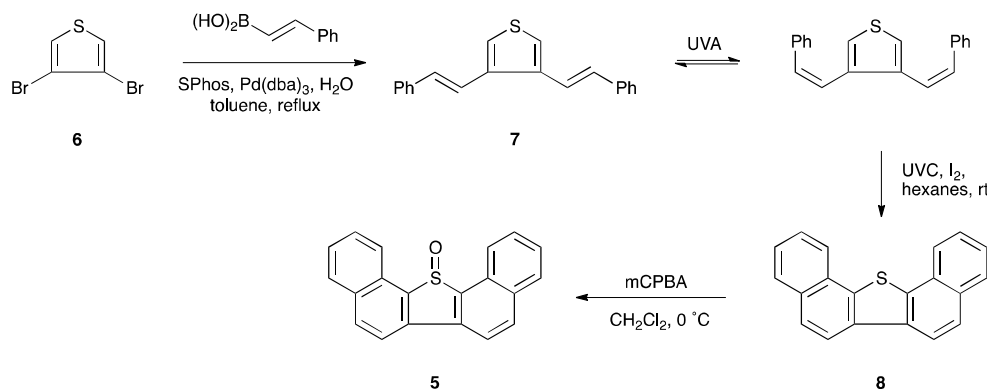
Determination of Quantum Yields

For quantum yields determined at 330 nm, a 75 W Xe lamp focused directly on a monochromator (Photon Technologies International) was used in most experiments. Slit widths were set to allow 6 nm linear dispersion. Samples of 4.0 mL in 1 cm square quartz cells were placed in a permanently mounted cell holder. The holder was placed such that all exiting light entered the sample cell without further focusing. All samples were sparged with argon (>20 minutes) prior to irradiation. All quantum yield experiments were carried out at a concentration high enough to reach an optical density >2 at the given wavelength and carried out to low conversion (<25%). Analysis of the reaction mixtures at various time points was performed and carried out with HPLC or GC analysis. Photolysis of azoxybenzene to yield the rearranged product, *o*-hydroxyazobenzene, was used as a chemical actinometer.²⁰

Product studies from steady state irradiations

For **DBTO** and **1-5**, solutions for irradiation with concentrations ranging from 1-6 mM were prepared. No significant variation in the observed yields was observed over this range of concentrations. Prior to irradiation, samples were degassed by argon sparging (≥20 minutes). The solutions were irradiated with 14 UVA bulbs (LZC-UVA, 8 watts, broad spectrum with λ_{max} = 350 nm) in a LZC-4X photoreactor from Luzchem. The conversion of **DBTO** and **1-5** to the corresponding thiophene was not allowed to exceed 30%. For analysis, dodecane was used as internal standard. Small samples were removed by syringe and subjected to HPLC or GC analysis.

Scheme 1



Computational Methods

Initial guess geometries were generated HF/6-31G(d) level of theory. To determine the redox potentials of the sulfoxides, the approach described by Davis and Fry was used.²¹ In this approach, the neutral species, radical cation, and radical anion of each compound were optimized separately using B3LYP/6-31G+(d) with SMD/IEF-PCM solvation in acetonitrile. Vibrational analysis was used to confirm the absence of imaginary frequencies and to determine the thermal free energies at 298.15 K. To determine excited-state energies, optimized geometries for the S_0 , S_1 , and T_1 were determined at the B3LYP/6-31G(d,p) or TD-B3LYP/6-31G(d,p) level of theory. Again, vibrational analysis was used to confirm the absence of imaginary frequencies and provide thermal corrections. To examine if a larger basis set or different levels of theory would improve performance, the energies at these geometries were further refined using M06-2X, CIS, or B3LYP level of theory with the aug-cc-pv(T+d)Z basis set.²² All geometry optimizations were performed with the Gaussian 09 or ORCA suite of programs.^{23,24}

Results and Discussion

Synthesis of Dinaphtho[2,1-b:1',2'-d]thiophene S-oxide (5).

Unlike the sulfoxides **1-4**, whose corresponding thiophenes were prepared by literature procedures,¹⁴⁻¹⁹ a new synthetic route was utilized to prepare **5**. As shown in Scheme 1, **5** was prepared in four steps from 3,4-dibromothiophene (**6**). The initial Suzuki-Miyaura coupling of **6** and *trans*-2-phenylvinylboronic acid was most efficient when using the ligand, 2-(2',6'-dimethoxybiphenyl)-dicyclohexyl-phosphine (SPhos). With these conditions, 3,4-bis-[(*E*)-2-phenylethenyl]-thiophene (**7**) was isolated with a moderate yield of 71.0%. The conversion of **7** to dinaphtho[2,1-b:1',2'-d]thiophene (**8**) involved a *trans* to *cis* conversion followed by a photoinduced electrocyclozation and oxidative aromatization. Side products observed during the photocyclization were reduced by first isomerizing **7** to the *cis*-conformations. Irradiation of **7** in hexanes using broadly emitting UVA bulbs (centered at $\lambda_{\text{max}} = 350$ nm) resulted in isomerization without cyclization. After isomerization, I_2 and propylene oxide were added to the solution, and then the solution was irradiated at 254 nm for one additional hour to induce

electrocyclozation and aromatization. Oxidation of **8** by mCPBA yielded **5**.

Photodexoygenation of 1-5

Photodeoxygenation of **1-5** was expected to generate $O(^3P)$ and the corresponding thiophene. To confirm this hypothesis, the oxidation products that arose from the irradiation of **DBTO** or **1-5** were compared. The enlarged chromophores of **1-5**, compared to the parent **DBTO**, were expected to red-shift their absorption spectra—potentially into the visible region, and further, to allow the photogeneration of $O(^3P)$ in samples containing compounds that absorb in the UV-A region of the spectrum without the complicating photochemistry.

UV-Vis Absorbance of 1-5. One of the main drawbacks of **DBTO** as a $O(^3P)$ precursor for applications in biological samples is the need for wavelengths below 350 nm to release $O(^3P)$. To examine the potential of **1-5** to generate $O(^3P)$ at longer wavelengths, the ground-state absorption spectra were obtained for **1-5** and are shown in Figure 1. In Figure 1(A), the absorption spectra of **1**, **2**, and **DBTO** are shown. Three absorption bands were observed for **DBTO** with the λ_{max} of the third band being 319 nm. For **1** and **2**, the λ_{max} of the longest wavelength band was 353 and 341 nm, respectively. Additionally, the extinction coefficient (ϵ) for **1** and **2** fell below 100 at 386 and 395 nm, respectively. As expected, the spectra of **1** and **2** extended past 350 nm; however, significant absorption for **1** and **2** did not extend into the visible.

The additional benzo moiety was expected to red-shift the longer wavelength band of **3-5** compared to **1** and **2**. The absorption spectra of **3-5** are shown in Figure 1(B). The sulfoxide **4** had the most red-shifted absorption spectrum. The λ_{max} of the longest wavelength band for **4** was 387 nm compared to 361 and 363 nm for **3** and **5**, respectively. The absorption of **4** extends the furthest into the visible region with its extinction coefficient (ϵ) falling below 100 at 437 nm compared to 419 and 423 nm for **3** and **5**, respectively.

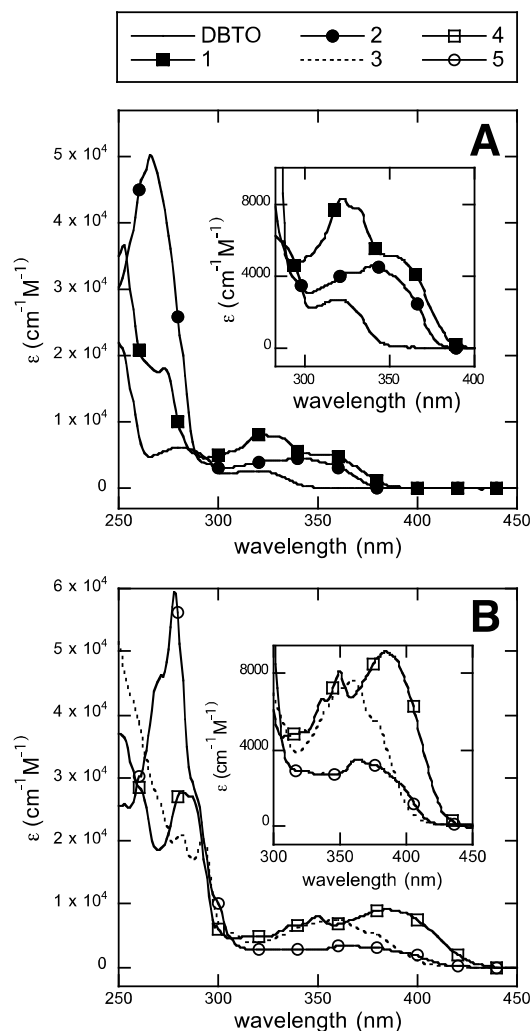


Figure 1. UV Spectra of the **DBTO** and thiophene *S*-oxides **1-5**. (A) UV Spectra of **DBTO** (solid line), **1** (solid line with closed square), and **2** (solid with closed circle) in acetonitrile. (B) UV Spectra of **3** (dotted line), **4** (solid line with open square), and **5** (solid line with open circle) in acetonitrile. Inserts depict expanded view of longer wavelengths.

Quantum Yields of Deoxygenation. The quantum yield of photodeoxygenation of **DBTO** has typically been found to range from 0.002 to 0.010 in different organic solvents.² Table 1 list the quantum yields for the deoxygenation of **1-5** irradiated at 330 nm in acetonitrile. To examine the photodeoxygenation, the quantum yield for the loss of **1-5** ($\Phi_{\text{-sulfoxide}}$) and the appearance of the corresponding thiophene ($\Phi_{\text{+sulfide}}$) were determined. The values ranged from 0.0095 to 0.0027 for $\Phi_{\text{-sulfoxide}}$ and 0.0078 to 0.0015 for $\Phi_{\text{+sulfide}}$. The quantum yields for the loss of sulfoxide ($\Phi_{\text{-sulfoxide}}$) and the formation of the corresponding thiophene ($\Phi_{\text{+sulfide}}$) were within the experimental error of each other. No other significant products were detected by HPLC or GC analysis. As expected, the photodeoxygenation of **1-5** directly resulted in the formation of corresponding thiophene as the only identifiable major product.

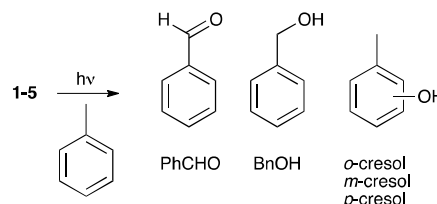
Table 1. Quantum Yield for the Deoxygenation of **1-5**.^a

Sulfoxide	λ (nm)	$\Phi_{\text{-sulfoxide}}$	$\Phi_{\text{+sulfide}}$
DBTO	320		0.0026 ± 0.0004^b
1	330	0.0040 ± 0.0001	0.0042 ± 0.0018
2	330	0.006 ± 0.003	0.0047 ± 0.0015
3	330	0.0095 ± 0.0005	0.0078 ± 0.0012
4	330	0.0027 ± 0.0018	0.0015 ± 0.0012
5	330	0.008 ± 0.004	0.0035 ± 0.0009

^a Quantum yields for the photodeoxygenation of thiophene *S*-oxides **1-5** all measured in acetonitrile. ^b **DBTO** photodeoxygenation quantum yield value from reference 2.

The quantum yields for deoxygenation for **1-5** are slightly higher than those for **DBTO**. The largest quantum yields values of 0.0095 for $\Phi_{\text{-sulfoxide}}$ and 0.0078 for $\Phi_{\text{+sulfide}}$ were observed for **3**.

Solvent Oxidation Products. Since $O(^3P)$ is difficult to detect, the yields of oxidized products have been used previously to indicate that the same oxidant was being produced.^{5,10,25} Yields of the oxidized products resulting from the irradiation of the parent **DBTO** in toluene were compared to previously reported studies.^{5,25} In our experiments, products arising from oxidation of the methyl group (PhCHO and BnOH) accounted for 8% of the oxidant produced in the photodeoxygenation of **DBTO**, and oxidation of the ring (*o*-cresol, *m*-cresol, and *p*-cresol) accounted for 38% as shown in Table 2. Previous studies have reported total yields of oxidized products as 73% and 78%, and thus, our total yield of 46% was considerably less. Additionally, the ratio of methyl to ring oxidation of 1:4.8 was less than the previously reported values of 1:2 and 1:1.6.



Comparison of our yields to those previously reported for **DBTO** indicate the yields of oxidized products are sensitive to the experimental conditions. Sensitivity to conditions is a common observation for the photodeoxygenation of **DBTO**. For example, the presence of molecular oxygen (O_2) can change the yields and ratio of oxidized products that accompany the photodeoxygenation of **DBTO** and its derivatives.^{5,11} Given the known sensitivity to experimental conditions, the yields obtained from the photodeoxygenation of **DBTO** in our experiments provided a suitable standard to compare yields obtained for compounds **1-5**.

Journal Name

ARTICLE

Table 2. Comparison of toluene oxidation product yields by **DBTO** and thiophene *S*-oxides **1-5**.^a

Sulfoxide	PhCHO	BnOH	o-cresol	m- & p-cresol ^b	Total %yield oxidized toluene	Oxidation CH ₃ :Ring ^c
DBTO ^d	14 ± 3	10 ± 1	25 ± 3	24 ± 6	73 ± 7	1 : 2.0
DBTO ^e	17 ± 3	13 ± 4	26 ± 5	22 ± 5	78 ± 9	1 : 1.6
DBTO ^f	3 ± 1	5 ± 1	20 ± 1	18 ± 1	46 ± 2	1 : 4.8
1 ^f	2.4 ± 0.5	5.1 ± 0.8	9.8 ± 0.8	5.6 ± 0.3	22.9 ± 1.3	1 : 2.0
2 ^f	1.7 ± 0.4	3.4 ± 0.6	5.5 ± 0.3	2.7 ± 0.2	13.3 ± 0.8	1 : 1.6
3 ^f	2.1 ± 0.5	4 ± 1	3.8 ± 0.9	2.4 ± 0.6	12.3 ± 1.6	1 : 1.0
4 ^f	8.3 ± 1.1	11.8 ± 1.8	2.8 ± 0.4	1.3 ± 0.2	24.2 ± 2.2	4.9 : 1
5 ^f	1.6 ± 0.2	2.2 ± 0.5	3.3 ± 0.0	2.4 ± 0.1	9.5 ± 0.5	1 : 1.5

^a Yields of toluene oxidation products relative to the formation of the corresponding sulfide of **DBTO** and thiophene *S*-oxides **1-5**. The oxidation products are benzaldehyde (PhCHO), benzyl alcohol (BnOH), and all three cresol isomers. ^b Measured as a single peak by GC-FID. ^c Ratio of PhCHO plus BnOH yields to combined cresol yields. ^d Values from reference 5. ^e Values from reference 25. ^f This work.

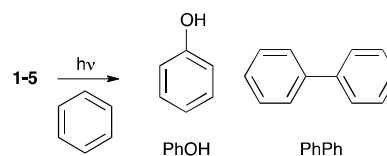
As shown in Table 2, a significant decrease in the total yield of oxidized toluene products for **1-5** compared to **DBTO** was observed. For **1-5**, the yield of all oxidized solvent products only accounted for 24.2% of the deoxygenation of **4** at the high end and ranged down to 9.5%, which was observed for **5**. This change represented a nearly 2-fold (at least) decrease compared to the 46% overall yield of oxidized solvent observed for **DBTO**. This decrease indicated a significant fraction, possibly all, of the photodeoxygenation of **1-5** occurs through a different mechanism than the parent **DBTO**.

The ratio of the oxidized solvent products was used to determine if a common oxidant was formed. With the notable exception of compound **4**, photodeoxygenation resulted in higher yields of ring oxidation products (cresols) than the combined methyl oxidation products (benzaldehyde and benzyl alcohol). The ratio of methyl oxidation products to cresols was 1:4.8 for **DBTO** in this work. The ratio of methyl to ring oxidation for the photodeoxygenation **1-5** ranged from 1:2 to 1:1 with notable exception of **4** whose ratio was 4.9:1. The change in the ratio of oxidized products suggested a fraction, possibly all, of the photodeoxygenation of **1-5** generating an oxidant that was different than the parent **DBTO**. However, the ratio of methyl to ring oxidation for **1-3** and **5** was similar to results previously reported for **DBTO** of 1:1.6 and 1:2.^{5,24} The errors associated with the ratio of oxidized solvent for **DBTO** and **1-5** were all insignificantly small, and thus, these errors were listed in Table S1 in the ESI.

As noted above, the ratio of benzaldehyde and benzyl alcohol to cresols was 4.9:1 for **4**, which was the reverse of all other examined thiophene *S*-oxides that yielded more cresols. Thus, the photodeoxygenation of **4** must proceed by a different mechanism, at least in part, than that of **DBTO**. Additionally, this mechanism

must have produced an oxidant or species that preferentially oxidized toluene to benzaldehyde or benzyl alcohol over cresols.

The yields of the oxidized solvent from the irradiation of **1-5** in toluene suggested the mechanism was different than that of **DBTO**. To confirm this result, **DBTO** and **1-5** were irradiated in benzene, and two oxidation products were observed: phenol and biphenyl.

**Table 3.** Comparison of benzene oxidation product yields by **DBTO** and thiophene *S*-oxides **1-5**.^a

Sulfoxide	Phenol	Biphenyl	Total	PhOH:PhPh
DBTO	34 ± 3	0.6 ± 0.1	35 ± 3	57:1
1	12.8 ± 0.6	0.6 ± 0.1	13.4 ± 0.6	21:1
2	14.3 ± 1.3	0.6 ± 0.1	14.9 ± 1.3	24:1
3	11.1 ± 0.8	0.8 ± 0.1	11.9 ± 0.8	14:1
4	7.2 ± 0.9	1.1 ± 0.2	8.3 ± 0.9	7:1
5	8.4 ± 0.4	0.7 ± 0.1	9.1 ± 0.4	12:1

^a Yields of benzene oxidation products relative to the formation of the corresponding sulfide of **DBTO** and the thiophene *S*-oxides **1-5**. The oxidation products were phenol and biphenyl.

For the oxidation of benzene, a similar trend as observed in the oxidation of toluene emerged. For **DBTO**, the formation of phenol

was favored over biphenyl in a ratio of 57:1 as shown in Table 3. For **1**, **2**, **3** and **5**, a more than 2-fold decrease compared to **DBTO** in the yield of phenol relative to the amount of deoxygenation was observed. Irradiation of **4** in benzene resulted in the lowest yield of phenol at 7.2% and highest yield of biphenyl at 1.1%. The ratio of 7:1 phenol to biphenyl for **4** was significantly different than all the other thiophene *S*-oxides examined. This trend was also consistent with a change in mechanism for the photodeoxygenation of **1-5**.

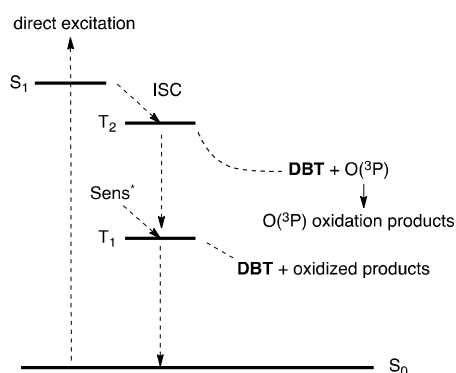
As will be discussed below, we posited this change was the emergence of two competitive deoxygenation mechanisms. The first mechanism being the release of $O(^3P)$ leading preferentially to oxygen insertion into arene C–H bonds and cresol formation. The second mechanism was postulated as being similar to triplet sensitized deoxygenation of **DBTO**.²⁵

Photodeoxygenation mechanisms

The results of the product studies indicated there was a change or emergence of a competing mechanism in the photodeoxygenation of **1-5** compared to **DBTO**. For **DBTO**, three distinct mechanisms of deoxygenation have been previously reported.^{2,25,26} Direct irradiation of **DBTO** has been posited to undergo a unimolecular S–O bond scission leading to **DBT** and $O(^3P)$. In addition to this unimolecular mechanism, bimolecular triplet sensitization and one-electron reduction of **DBTO** have also been shown to result in deoxygenation. Given the structural similarity of **1-5** to **DBTO**, it was hypothesized the change in solvent oxidation products for **1-5** was the result of a mechanism similar to triplet sensitized or one-electron reduction mechanisms becoming competitive or dominant over the release of $O(^3P)$.

Direct irradiation of DBTO. In organic solvents, the deoxygenation of **DBTO** by direct irradiation has been postulated to occur via dissociative T_2 state. This mechanism was based on CAS/SCF and MRMP2 calculations.²⁷ These calculation demonstrated the T_2 state of thiophene *S*-oxides dissociates to the corresponding thiophene and $O(^3P)$. At the S_1 optimized geometry, the energy of T_2 was below that of S_1 which indicated intersystem crossing (ISC) from S_1 to T_2 was energetically feasible. Additionally, a considerable barrier to S–O cleavage along the T_1 surface was found. Thus, the mechanism for $O(^3P)$ generation was proposed to result from the direct excitation into the S_1 state of **DBTO** followed by ISC into the dissociative T_2 state as shown in Scheme 2.

Scheme 2. Potential deoxygenation mechanisms for **DBTO**.



Triplet sensitized photodeoxygenation of DBTO. Deoxygenation of **DBTO** has also been induced by selective irradiation of common triplet sensitizers, namely anthraquinone and benzophenone, in toluene.²⁵ Yields of the **DBT** ranged from 83 to 94%, and the toluene oxidation products of PhCHO, BnOH, and all three cresol isomers were observed. The ratio of the products arising from methyl oxidation (PhCHO and BnOH) and ring oxidation (cresols) was compared to those obtained by the direct irradiation of **DBTO**. Direct irradiation of **DBTO** resulted in a ratio of 1:1.6 for CH_3 versus ring oxidation; however, the ratio was reversed when a triplet sensitizer was used. The ratio of CH_3 :ring oxidation was 3.5:1 for anthraquinone and 8.1:1 for benzophenone, which was similar to the 4.9:1 ratio observed for **4**. Additionally, the overall yields of toluene oxidation products dropped substantially in the sensitized conditions compared to direct irradiation. This led to the conclusion that the mechanism of **DBTO** deoxygenation in direct and sensitized conditions were different. The sensitized mechanism was believed to occur through the T_1 state as shown in Figure 1.

Bimolecular photoreduction photodeoxygenation of DBTO. In the presence of methoxide, photoinduced one-electron transfer from methoxide to **DBTO** or any aryl sulfoxide was believed to initiate deoxygenation. The resulting 9-S-3 hydroxysulfuranyl radical anion, of the sulfoxide was believed to protonate and undergo a heterolytic S–O bond cleavage. Further evidence for this mechanism was obtained by selectively irradiating *N*-methylcarbazole, a known electron donor, in the presence of **DBTO** to generate the 9-S-3 hydroxysulfuranyl radical anion.

The working hypothesis for the change in solvent oxidation for **1-5** was that a mechanism similar to the triplet sensitized or one-electron reduction mechanism was competitive with or dominant over the release of $O(^3P)$. To gain insight into this possibility, redox and excited state properties of **1-5** and **DBTO** were examined with computational methods.

Computed Properties of DBTO and thiophenes 1-5

One potential cause for the difference in the direct irradiation of **DBTO** and **1-5** would be a change in the excited state energies. Differences in the excited energies of **1-5** could change the partitioning into T_1 and T_2 and account for the observed difference in product yields. For example, an increase in the state energy of T_2 could make it inaccessible from the S_1 state. To examine if the excited state energies of **1-5** were different than **DBTO** TD-DFT methods were used.

Computed Excited State Energies. The S_1 and T_1 energies of **DBTO** were previously determined from its fluorescence and phosphorescence spectra.²⁸ The S_1 energy of **DBTO** was determined from the red-edge of the fluorescent spectra as 85 kcal mol⁻¹. The T_1 energy of **DBTO** was determined from the phosphorescence spectra of **DBTO** in ether/isopentane/ethanol (EPA) at 77 K as 61 kcal mol⁻¹. Given the size of thiophene *S*-oxides **3-5** and available computational resources, the ability of TD-DFT and CIS methods to obtain suitable excited state energies within a reasonable time was evaluated.

The ability of several computational methods to predict the excited state energies of **DBTO** was examined by comparing the computed and experimental values. To these ends, TD-B3LYP and B3LYP with

the 6-31G(d,p) basis set were used to find the optimized geometries for the S_0 , S_1 , and T_1 states of **DBTO**. For accurate energies of sulfur containing molecules, a large basis set is often needed.²⁹⁻³² Thus, energies at the B3LYP/6-31G(d,p) structures were further refined using the M06-2X, B3LYP, and CIS levels of theory with the aug-cc-pV(T+d)Z basis set.^{22,33} The predicted S_1 and T_1 energies are shown in Table 4.

Table 4. Comparison of computed S_1 and T_1 energies of **DBTO** to the experimentally determined values.^a

Method	S_1	T_1
B3LYP/6-31G(d,p)	70	63
B3LYP/aug-cc-pV(T+d)Z//B3LYP/6-31G(d,p)	72	62
M06-2X/aug-cc-pV(T+d)Z//B3LYP/6-31G(d,p)	83	70
CIS/aug-cc-pV(T+d)Z//B3LYP/6-31G(d,p)	112	80
Experimental ^b	85	61

^a S_1 and T_1 energies in kcal mol⁻¹ for **DBTO** determined from the difference between the excited and ground (S_0) state energies (H at 0 K) at a given level of theory. ^b Experimental S_1 and T_1 energies from reference.³⁴

The predicted S_1 and T_1 energies at the B3LYP/6-31G(d,p) level of theory were 70 and 63 kcal mol⁻¹, respectively. It was anticipated a larger basis set with large exponential d -functions like aug-cc-pV(T+d)Z would better replicate the experimentally determined excited state energies. However, only a marginal improvement was observed with the S_1 and T_1 energies being 72 and 62 kcal/mol. Switching to the M06-2X functional with the aug-cc-pV(T+d)Z basis set yielded energies of 83 and 70 kcal mol⁻¹, which was not considered a significant improvement. Finally, the CIS/aug-cc-pVT+dZ level of theory had poor performance predicting values of 112 and 80 kcal mol⁻¹ for the S_1 and T_1 state energies, respectively.

None of the examined computational methods were likely to give quantitatively valuable predictions of the excited energies of **1-5**. More expensive computational methods such as MRMP2, have provided reliable estimates of the T_1 state energy for **DBTO**; however, the predicted S_1 energy was off by 7 kcal mol⁻¹ or more.²⁷ Thus, using more computationally expensive methods such as MRMP2 or CASSCF were not likely to improve the predicted values. Given the additional computational cost of the aug-cc-pV(T+d)Z basis set, the B3LYP/6-31G(d,p) level of theory was used to examine the excited state energies of **1-5** for any qualitatively useful trends.

The excited state energies of **DBTO** and **1-5** are given in Table 5. While a stable minima for the S_0 , S_1 , and T_1 states were found, all attempts to find a stable T_2 geometry resulted in the S–O bond scission. This was expected due to the dissociative T_2 state of **DBTO**. The predicted S_1 energies of **1-5** were relatively similar, ranging from 65.8 to 62.3 kcal mol⁻¹, which was slightly lower than the 70.0 kcal mol⁻¹ for **DBTO**. The T_1 energies of **1-5** were lower than those found for **DBTO**. The most striking difference was the T_1 energies of **1-5** were all more than 10 kcal mol⁻¹ lower than for **DBTO**. This resulted in much larger S_1 - T_1 gap for **1-5**, which ranged 13.5 to 20.1 kcal mol⁻¹, which was much larger than the 7.0 kcal mol⁻¹ gap for

DBTO. While the predicted excited state energies were unlikely quantitatively accurate, the substantial S_1 - T_1 energy gap for **1-5** compared to **DBTO** was a consistent feature.

Table 5. TD-B3LYP and B3LYP/6-31G(d,p) excited state energies relative to S_0 .

Sulfoxide	S_1^a	T_1^a	ΔE_{ST}^b
DBTO	70.0	63.0	7.0
1	65.0	49.4	15.6
2	65.8	52.3	13.5
3	64.8	48.0	16.8
4	62.3	42.2	20.1
5	62.7	49.0	13.7

^a S_1 and T_1 energies in kcal mol⁻¹ determined from the difference between the excited and ground (S_0) state energies (H at 0 K) at B3LYP/6-31G(d,p) level of theory. ^b S_1 - T_1 energy gap in kcal mol⁻¹.

The larger S_1 - T_1 energy gap for **1-5** compared to **DBTO** could affect the partitioning into the T_1 state versus the release of $O(^3P)$ from the T_2 state. The more exothermic intersystem crossing (ISC) from S_1 to T_1 or relaxation from T_2 could promote partitioning into the T_1 state. Notably, the largest S_1 - T_1 energy gap was found for **4** whose deoxygenation resulted in preferential benzyl oxidation, which was identical to the oxidation pattern observed for triplet sensitized **DBTO** deoxygenation. Thus, the larger S_1 - T_1 energy gap appeared to favor deoxygenation through an alternate mechanism at the expense of $O(^3P)$ generation for **1-5**.

As stated previously, attempts to find a stable T_2 geometry failed since T_2 was a dissociative state of **DBTO**. Since partitioning into T_2 was the proposed mechanism of $O(^3P)$ generation, a change in the relative energy gap between T_2 and S_1 or T_1 could affect the release of $O(^3P)$. For example, an increase in the T_2 energy relative to S_1 or potentially T_1 for **1-5** would be expected to disfavor $O(^3P)$ release compared to **DBTO**. To examine this possibility, T_2 energies at the optimized geometries of S_0 , S_1 and T_1 were determined. These energies are listed in Table S2 in the ESI. For **1-3**, T_2 was higher in energy than S_1 at all three geometries, and the relative energy of T_2 compared to S_1 and T_1 at all three geometries was similar to **DBTO**.

Sulfoxides **4** and **5** were exceptions. For sulfoxides **4** and **5**, the T_2 was 2-5 kcal mol⁻¹ lower than the S_1 at the T_1 geometry, and the T_2 energies were consistently lower for **4** and **5** when compared to **1-3** and **DBTO** at all geometries. However, it was unclear if this was a significant result. While the methyl to ring oxidation ratio listed in Table 2 is different for **4** compared to **1-3** and **DBTO**, the 1:1.5 ratio for **5** is similar the other sulfoxides. If the lower T_2 energies for **4** and **5** were significant, it would be expected that **4** and **5** would have displayed similar oxidation product ratios. Thus, it was unclear if any mechanistic insight could be gained from this data.

Excited state energies and solvent oxidation products of **4** were substantially different than those compared to **1-3**, **5** and **DBTO**. Unlike the **1-3**, **5** and **DBTO** that have relatively flat structures, the B3LYP/6-31G(d,p) ground-state optimized structure of **4** was twisted as shown in Figure 2. The dihedral angle between the

ARTICLE

Journal Name

naphthyl moieties ($C_x-C-C-C_y$) was 24.2° for **4**. The corresponding dihedral for **DBTO**, **1** and **5** was near zero, and the dihedral for **1** and **3** was 6.2° and 13.2° , respectively (data given in ESI).

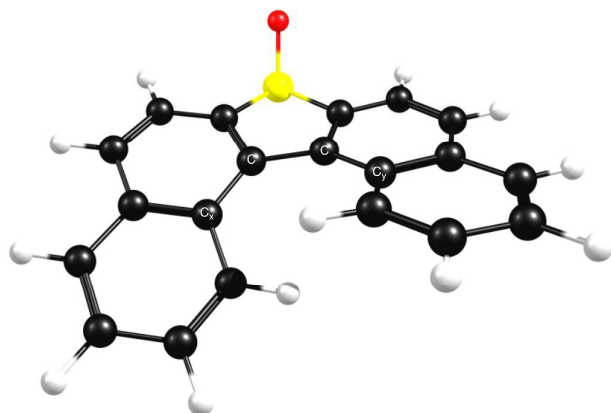


Figure 2. B3LYP/6-31G(d,p) optimized structure of **4** showing $C_x-C-C-C_y$ dihedral angle of 24.2° . Carbon=Black, White=Hydrogen, Yellow=Sulfur, Red=Oxygen.

Computed Redox potentials. An increased susceptibility to photoinduced electron transfer was an alternative possibility to $O(^3P)$ release, which could explain the difference in solvent oxidation patterns for **1-5** compared to **DBTO**. Davis and Fry have shown that B3LYP can be used to accurately predict hydrocarbon arene redox potentials.²¹ Following the method described by Davis and Fry, the ionization potential and electron affinity of benzene, naphthalene, chrysene, pyridine, pyrrole, pyrimidine, quinolone, and thiophene were determined to examine if this method could be applied to heteroaromatic compounds. While additional sulfur containing aromatic heterocycles would have been desirable for this test set, the selected molecules were chosen since their oxidation potentials had been determined under similar experimental conditions.^{35,36} Figure 3 illustrates the correlation between the computationally predicted and experimentally determined redox values for the test set.

As shown in Figure 3(A), correlation between the predicted and experimental oxidation potential for the hydrocarbons (benzene, naphthalene, chrysene) was excellent ($R=0.9991$). This was consistent with the findings of Davis and Fry.²¹ Comparison of the hydrocarbons plus thiophene, pyridine, and pyrrole was worse with a correlation coefficient of 0.91121. Correlation between experimentally determined reduction potential and computationally determined electron affinities was decent with a correlation coefficient of 0.98844. This was considered sufficient to determine if the redox potentials of **1-5** were drastically different than **DBTO**.

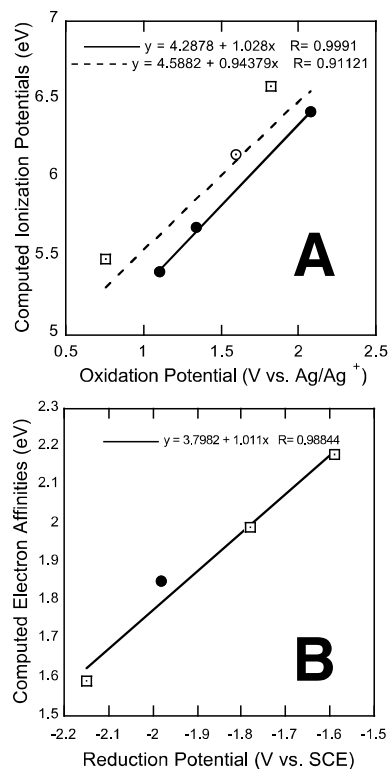


Figure 3. Comparison of PCM-B3LYP/6-31+G(d) estimated potential to those determined by polarography or cyclic voltammetry. Closed circles: (hydrocarbon aromatics, benzene, naphthalene and chrysene); Open circle (thiophene); Open square: (nitrogen-containing aromatics, pyridine, pyrrole, quinoline, pyrimidine). **(A)** Ionization potentials compared to oxidation potential determined in reference 35. Regression analysis: solid line (only hydrocarbon aromatics); dotted line (all compounds). **(B)** Comparison of PCM-B3LYP/6-31+G(d) estimated electron affinities to reduction potential determined by polarography in reference 36.

Table 6. The computed redox potential for **DBTO** and **1-5**.

Sulfoxide	IP (eV)	EA (eV)
DBTO	6.27	2.33
1	5.66	2.63
2	5.77	2.60
3	5.64	2.72
4	5.45	2.78
5	5.62	2.28

^a absolute reduction and ionization potentials computed by density functional theory (B3LYP/6-31+G(d)) with SMD/IEF-PCM solvation.

Table 6 lists the redox potentials of **1-5** and **DBTO** determined by following the method described by Davis and Fry.²¹ The ionization potentials of **1-5** ranged from 5.77 to 5.45, which was lower than the 6.27 eV value for **DBTO**. The electron affinities (EA) of **1-5** ranged from 2.72 to 2.28. If **1-5** were more susceptible to reduction

than **DBTO**, the electron affinity of **1-5** would be significantly larger than **DBTO**. The EA of **DBTO** was 2.33, which fell in the middle of the range of EA for **1-5**. Thus, it was concluded that bimolecular photoreduction was not responsible for the different oxidation pattern observed for **1-5**.

Photodeoxygenation mechanism of 1-5

The product studies and computed properties of **1-5** indicated deoxygenation occurred by two different mechanisms. Deoxygenation of **DBTO** has been proposed to occur by both the T_2 and T_1 states. The dissociative T_2 state leads to $O(^3P)$, which selectively oxidized toluene to cresols. Under bimolecular triplet sensitized conditions which presumably bypass the T_2 state, deoxygenation from the T_1 state was shown to result in a decrease in the overall oxidation of toluene and preferential oxidation of the benzylic position.²⁵

The direct irradiation of **1-5** also resulted in a decrease in the yields of toluene oxidation products. However, unlike the triplet sensitization of **DBTO** that leads preferentially to methyl oxidation products, cresols were the major oxidation products from the deoxygenation of **1-3** and **5**. This suggested that **1-5** were undergoing deoxygenation by two competing mechanisms. One mechanism generates $O(^3P)$, presumably through a T_2 state, and the second mechanism appeared similar to triplet sensitization of **DBTO** which does not generate $O(^3P)$ and proceed through a T_1 state. Thus, the variations in the oxidation yields between **1-5** were the result of differing partitioning into these two competing mechanisms. For example, the benzyl:ring oxidation of **1** is 1:2, which is the most similar to that of 1:4.8 for **DBTO**, which presumably produces the most $O(^3P)$. However, the total yield of toluene oxidation relative to the formation of the corresponding sulfide of **1** dropped to 23% compared to 48% for **DBTO**. This drop indicates **1** also undergoes deoxygenation through the T_1 state or a mechanism similar to one arising from triplet sensitization. This T_1 mechanism must also lead to an oxidant or species that preferentially generates PhCHO and BnOH in low yields. This concomitantly resulted in a lower yield of $O(^3P)$ which preferentially oxidized toluene to the cresol products. Thus, the drop in total oxidation and slightly smaller ratio of benzyl:ring oxidation is consistent with **1** undergoing both mechanisms.

As stated earlier, the direct irradiation of **4** resulted in PhCHO and BnOH as the major products. This was a similar ratio of benzyl:ring oxidation that was observed during the photosensitized deoxygenation of **DBTO**. This led to the conclusion that **4** may not generate any $O(^3P)$ and exclusively undergo deoxygenation through the surmised T_1 mechanism. Computed properties found the T_1 energy of **4** was significantly lower than all the other thiophene S -oxides in the study. This could account for a greater partitioning into the T_1 state of **4** and deoxygenation without releasing $O(^3P)$.

Conclusions

The photodeoxygenation of thiophene S -oxides **1-5** was investigated. While **1-5** absorbed longer wavelengths compared to **DBTO**, oxidation of toluene and benzene during the irradiation of **1-5** yielded product ratios different from

DBTO. This indicated the photodeoxygenation of **1-5** and **DBTO** occurred by two different mechanisms. For **DBTO**, photodeoxygenation occurred primarily through a dissociative T_2 state to release $O(^3P)$. In the oxidation of toluene, this resulted in cresols being the major products. For **1-5**, a competitive deoxygenation mechanism through the T_1 state, which favored oxidation of the benzylic position of toluene, was presumed. Larger computed S_1 - T_1 energy gaps favored deoxygenation through the T_1 mechanism, and **4** was believed to largely undergo deoxygenation by this mechanism.

Acknowledgements

Portion of this work was supported by the National Science Foundation under CHE-1255270. The authors thank the National Science Foundation for support under grant CHE-0963363 for renovations to the research laboratories in Monsanto Hall. This work was additionally supported by donors to the Herman Frasch Foundation.

Notes and references

- Z. Wan and W. Jenks, *J. Am. Chem. Soc.*, 1995, **117**, 2667–2668.
- D. Gregory, Z. Wan and W. Jenks, *J. Am. Chem. Soc.*, 1997, **119**, 94–102.
- E. Lucien and A. Greer, *J. Org. Chem.*, 2001, **66**, 4576–4579.
- K. B. Thomas and A. Greer, *J. Org. Chem.*, 2003, **68**, 1886–1891.
- R. D. McCulla and W. S. Jenks, *J. Am. Chem. Soc.*, 2004, **126**, 16058–16065.
- M. Nag and W. S. Jenks, *J. Org. Chem.*, 2004, **69**, 8177–8182.
- M. Nag and W. S. Jenks, *J. Org. Chem.*, 2005, **70**, 3458–3463.
- G. Bucher and J. Scaiano, *The Journal of Physical Chemistry*, 1994, **98**, 12471–12473.
- M. Zhang, G. E. Ravilious, L. M. Hicks, J. M. Jez and R. D. McCulla, *J. Am. Chem. Soc.*, 2012, **134**, 16979–16982.
- J. Korang, W. R. Grither and R. D. McCulla, *J. Am. Chem. Soc.*, 2010, **132**, 4466–4476.
- M. T. Bourdillon, B. A. Ford, A. T. Knulty, C. N. Gray, M. Zhang, D. A. Ford and R. D. McCulla, *Photochem. Photobiol.*, 2014, **90**, 386–393.
- O. R. Wauchope, S. Shakya, N. Sawwan, J. F. Liebman and A. Greer, *J. of Sulfur Chem.*, 2007, **28**, 11–16.
- J. Korang, I. Emahi, W. R. Grither, S. M. Baumann, D. A. Baum and R. D. McCulla, *RSC Adv.*, 2013, **3**, 12390–12397.
- Y. Tominaga, M. L. Lee and R. N. Castle, *J. Heterocyclic Chem.*, 1981, **18**, 967–972.
- S. F. Nelsen, Y. Luo, M. N. Weaver, J. V. Lockard and J. I. Zink, *J. Org. Chem.*, 2006, **71**, 4286–4295.
- B. Rungtaweevoranit, A. Butsuri, K. Wongma, K. Sadorn, K. Neraanon, C. Nerungsi and T. Thongpanchang, *Tet. Lett.*, 2012, **53**, 1816–1818.
- S. M. Rafiq, R. Sivasakthikumar and A. K. Mohanakrishnan, *Org. Lett.*, 2014, **16**, 2720–2723.
- N. C. de Lucas, A. C. C. Albuquerque, A. C. A. S. Santos, S. J. Garden and D. E. Nicodem, *J. Photochem. Photobiol. A*, 2007, **188**, 293–297.
- A. Buquet, A. Couture, A. Lablache-Combiere and A. Pollet, *Tetrahedron*, 1981, **37**, 75–81.

ARTICLE

Journal Name

- 20 N. J. Bunce, J. LaMarre and S. P. Vaish, *Photochem. Photobiol.*, 1984, **39**, 531–533.
- 21 A. P. Davis and A. J. Fry, *J. Phys. Chem. A*, 2010, **114**, 12299–12304.
- 22 C. W. Bauschlicher and H. Partridge, *Chem. Phys. Lett.*, 1995, **240**, 533–540.
- 23 Gaussian 09, Revision E.01 M. J. Frisch, G. W. Trucks, H. B. Schlegel, G. E. Scuseria, M. A. Robb, J. R. Cheeseman, G. Scalmani, V. Barone, B. Mennucci, G. A. Petersson, H. Nakatsuji, M. Caricato, X. Li, H. P. Hratchian, A. F. Izmaylov, J. Bloino, G. Zheng, J. L. Sonnenberg, M. Hada, M. Ehara, K. Toyota, R. Fukuda, J. Hasegawa, M. Ishida, T. Nakajima, Y. Honda, O. Kitao, H. Nakai, T. Vreven, J. A. Montgomery Jr, J. E. Peralta, F. Ogliaro, M. J. Bearpark, J. Heyd, E. N. Brothers, K. N. Kudin, V. N. Staroverov, R. Kobayashi, J. Normand, K. Raghavachari, A. P. Rendell, J. C. Burant, S. S. Iyengar, J. Tomasi, M. Cossi, N. Rega, N. J. Millam, M. Klene, J. E. Knox, J. B. Cross, V. Bakken, C. Adamo, J. Jaramillo, R. Gomperts, R. E. Stratmann, O. Yazyev, A. J. Austin, R. Cammi, C. Pomelli, J. W. Ochterski, R. L. Martin, K. Morokuma, V. G. Zakrzewski, G. A. Voth, P. Salvador, J. J. Dannenberg, S. Dapprich, A. D. Daniels, Ö. Farkas, J. B. Foresman, J. V. Ortiz, J. Cioslowski and D. J. Fox, Gaussian, Inc., Wallingford CT, 2009.
- 24 F. Neese, *WIREs Comput. Mol. Sci.*, 2011, **2**, 73–78.
- 25 E. M. Rockafellow, R. D. McCulla and W. S. Jenks, *J. Photochem. Photobiol. A*, 2008, **198**, 45–51.
- 26 J. Cubbage, T. Tetzlaff, H. Groundwater, R. D. McCulla, M. Nag and W. Jenks, *J. Org. Chem.*, 2001, **66**, 8621–8628.
- 27 S. A. Stoffregen, S. Y. Lee, P. Dickerson and W. S. Jenks, *Photochem. Photobiol. Sci.*, 2014, **13**, 431.
- 28 W. Jenks, W. Lee and D. Shuttters, *J. Phys. Chem.*, 1994, **98**, 2282–2289.
- 29 D. D. Gregory and W. S. Jenks, *J. Org. Chem.*, 1998, **63**, 3859–3865.
- 30 O. Ventura, M. Kieninger, P. Denis and R. Cachau, *Chem. Phys. Lett.*, 2002, **355**, 207–213.
- 31 N. Wang and A. Wilson, *J. Phys. Chem. A*, 2003, **107**, 6720–6724.
- 32 J. Korang, W. R. Grither and R. D. McCulla, *J. Phys. Chem. A*, 2011, **115**, 2859–2865.
- 33 T. Dunning, K. Peterson and A. Wilson, *J. Chem. Phys.*, 2001, **114**, 9244–9253.
- 34 Y. Guo and W. S. Jenks, *J. Org. Chem.*, 1995, **60**, 5480–5486.
- 35 K. B. Wiberg and T. P. Lewis, *J. Am. Chem. Soc.*, 1970, **92**, 7154–7160.
- 36 J. W. Loveland and G. R. Dimeler, *Anal. Chem.*, 1961, **33**, 1196–1201.